Journal of the Korean Astronomical Society
51: 207 ∼ 214, 2018 December

https://doi.org/10.5303/JKAS.2018.51.6.207
pISSN: 1225-4614 · eISSN: 2288-890X
http://jkas.kas.org

Development of the SNU Coelostat: Conceptual Design

Juhyung Kang[1], Jongchul Chae[1], Hannah Kwak[1], and Heesu Yang[2]
[1]Department of Physics and Astronomy, Seoul National University, Gwanak-gu, Seoul 08826, Korea
jhkang@astro.snu.ac.kr
[2]Korea Astronomy and Space Science Institute, 776 Daedukdae-ro, Yuseong-gu, Daejeon 34055, Korea

Received October 10, 2018; accepted December 12, 2018

Abstract: A coelostat is often used for solar observations, because it corrects the image rotation automatically by guiding sunlight into a fixed telescope with two plane mirrors. For the purposes of education and spectroscopic observation, the solar group at Seoul National University (SNU) plans to develop the SNU coelostat (SNUC) and install it in the SNU Astronomical Observatory (SAO). Requirements of the SNUC are $< 1''$ positioning accuracy with 30 cm beam size on the entrance pupil in the compact dome. To allow for installation in the small dome, we design a compact slope type coelostat with a 45 cm primary plane mirror and a 39 cm secondary plane mirror. The motion of the SNUC is minimized by fixing the position of the slope frame. Numerical simulations of the available observational time of the designed coelostat shows that the sun can be observed ay all times from June to early August and at least three hours in other months. Since the high accuracy driving motors installed in the SNUC can be affected by external environment factors such as humidity and temperature variations, we design a prototype to test the significance of these effects. The prototype consists of a 20 cm primary plane mirror, a 1 m slope rail, a direct drive motor, a ballscrew, a linear motion guide, an AC servo motor, a reduction gear and a linear encoder. We plan to control and test the accuracy of the prototype with varying atmospheric conditions in early 2019. After testing the prototype, the SNUC will be manufactured and installed in SAO by 2020.

Key words: instrumentation: coelostat — Sun: general

1. Introduction

A high-resolution solar telescope is usually designed with a long focal length. Since long focal length telescopes are difficult to steer, some observatories use heliostats, coelostats, turrets or Coudé arrangements to guide the sunlight into fixed telescopes (Dunn 1985; Stix 2004). For the case of the heliostat or turret systems, the solar image on the focal plane is rotated. To correct the image rotation, observed data are de-rotated using a software (e.g., Maurya et al. 2013), or an additional counter rotating mirror is required. In some cases, Coudé laboratories are designed to be rotated (e.g., Dreyer et al. 2014). On the other hand, a coelostat makes an irrotational solar image by using an arrangement of two plane mirrors; the primary flat (PF) which rotates around the polar axis, and the secondary flat (SF) which redirects the sunlight into the fixed laboratory (Mills 1985). For this reason, a coelostat has been used for various high-resolution spectroscopic observations, such as the Vacuum Tower Telescope (VTT, Livingston et al. 1976) and the KASI Solar Imaging Spectrograph (KSIS, Park et al. 2003; Kim et al. 2006).

A coelostat has also been used to test instruments and present real-time solar images to the public. For the purpose of verification of an instrument, a coelostat has been used to test the transmission of filters (e.g., Park et al. 2003) and the driving of a spectropolarimeter or imaging spectrograph (e.g., Nah et al. 2011). Furthermore, a payload that is intended to be installed in a satellite can be tested in the laboratory using a coelostat, and also data obtained from a coelostat can be used to interpret spacecraft data (e.g., Livingston et al. 1976). A coelostat installed in the solar tower at Monte Mario shows real-time solar images and spectra to the public for educatial purposes (D'Allesio et al. 2012). Interestingly, after the completion of solar observation of the Linde-Robinson coelostat at Caltech, the reflected sunlight has subsequently been used for interior lighting (Han et al. 2014).

The astronomy group at Seoul National University (SNU) recently reconstructed the decrepit SNU Astronomical Observatory (SAO) and its facilities. For the purpose of solar observation, we plan to develop the SNU Coelostat (SNUC) and install it in the solar dome of the SAO by 2020. Moreover, we also plan to develop a prototype of the SNUC to verify the design procedures and conduct environmental tests. Since we are interested in photospheric and chromospheric events, the back-instrument (telescope) will consist of a white light photospheric filter and Hα chromospheric filter. The real time solar image will be shown in the large size imaging plate ($\geq$ 20 cm) and also the spectrum will be measured using slit or fiber. Details of the optics of the back-instrument will be reported in a subsequent paper.

The SNUC will provide students not only the op-

Corresponding author: J. Chae

Figure 1. The reconstructed SAO. The large dome located to the right is for night observations and includes the 1 m reflective telescope. The left dome is the solar dome, where the coelostat will be installed.

portunity to observe the solar spectrum and image simultaneously, but also be an educational venue where students can see optical systems and adjust them. Furthermore, the SNUC can be used to test both ground based optical instruments and space telescopes. This project is meaningful for graduate students in the solar group at SNU as all of the development processes, from design to control, will be conducted by them. By participating in this project, they can accumulate experience in developing instruments.

In Section 2, we describe the details of the SAO. We report the conceptual and mathematical design of the SNUC in Section 3. The design and details of the prototype of SNUC (PSNUC) are described in Section 4. A brief summary and future plan are provided in Section 5.

2. OBSERVATORY

The old SAO was used for education and research from 1978 until 2015. Due to decrepitudes of facilities, the SAO was recently reconstructed with high tech instruments for high-quality education and research (see Figure 1). The new SAO operates a remote observation system on the first floor and a 1 m telescope for night observation on the second floor, with the 8 m diameter hemispheric dome above this room. On the second floor, two optical tables are installed in the solar laboratory for the purpose of solar observations. The dimension of the laboratory is 3.5 m × 7.8 m, and the dimension of the optical tables are 1.2 m × 2 m. To reduce local turbulence inside the laboratory by maintaining the temperature and humidity, a cleanroom-based thermo-hygrostat has been installed.

Figure 2 shows the solar dome and laboratory. The sunlight (orange lines) is fed into the laboratory from the two coelostat mirrors, the PF (blue ellipse) and the SF (red ellipse) installed in the 3.5 m hemispheric dome above the laboratory. The optics is represented in the red dashed box. The sunlight passes through the objective lens on the top of the laboratory and gets reflected into the eyepiece by the plane mirror (green ellipse), forming the solar image on the imaging plate that has a diameter of 20 cm. This descrption of the optics is a simplified version, and more details will be provided in a subsequent paper.

Table 1
Information on the solar observational facilities

Parameter	Value
Outer diameter	ϕ 3.5 m
Inner diameter	ϕ 3 m
Height of the wall	0.8 m
Diameter of the hole	ϕ 0.6 m
Size of the laboratory	3.5 m × 7.8 m

Unlike the general sliding dome, the 3.5 m solar dome has four automatic hinged windows to reduce the local turbulence inside the dome by circulating the air inside and outside. The effective area inside the dome is 3 m since the thickness of the wall is approximately 25 cm. To feed the sunlight into the solar laboratory on the second floor, a 0.6 m diameter hole is perforated at the center of the floor inside the dome. The solar dome is located 1.16 m west and 0.04 m north from the 8 m dome.

Table 1 summarizes the observatory information of the solar dome and laboratory. Note that these parameters are important considerations when selecting the type of coelostat and its size.

3. CONCEPTUAL DESIGN OF THE SNUC

3.1. Requirements

There are three different types of coelostats; vertical, horizontal and slope. In the case of vertical type coelostat, the SF moves up and down as the declination of the Sun varies through the year. The SF is located at the highest level at the winter solstice and is at the lowest height at the summer solstice. Since the position of the PF is fixed, the SF only rotates on one axis. Different from the vertical type, the SFs of the other two types are fixed, and the positions of the PFs are changed maintaining their polar inclination. The main advantage of the horizontal type is that it is relatively easy to move the PF since it is not affected by gravity, which only contributes to the friction. The distance between the PF and SF, for the case of the horizontal type, is short in the winter and long in the summer. The slope type is the most compact among three; the distance between the PF and SF is constant for all seasons, and this type has the shortest mean distance between the two mirrors (see Figures 10–12 in Mills 1985). Among these three types of coelostats, we have to choose one that satisfies the following five requirements.

First, the coelostat has to be sufficiently compact to be placed in the dome. Since the inner diameter of the solar dome is 3 m, the horizontal length of the rail of the PF must be less than 1.5 m to allow sunlight to enter the dome without obstructing the hole. In addition, the height of the PF and the SF should be less than 2.3 m since the height of the wall is 0.8 m.

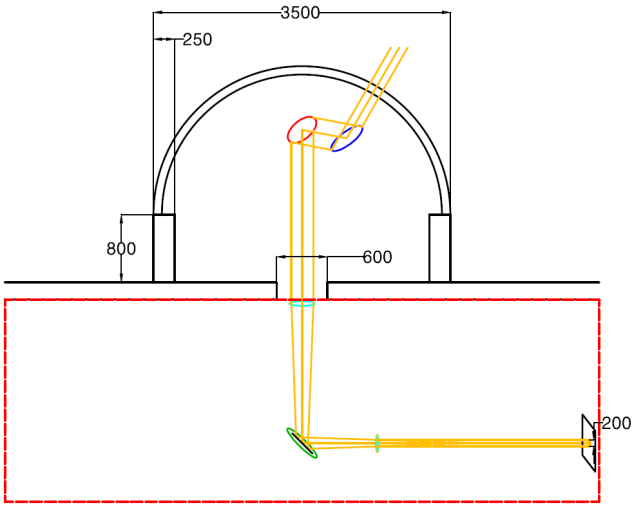

Figure 2. Schematic illustration of the solar dome and laboratory. Units of lengths are mm. The solar dome is shown in black line. The red (blue) ellipse represents the PM (SM) and the orange lines are the light path of the sunlight. The simplified optics are shown in the red dashed box.

Second, the required beam size on the entrance pupil is approximately 30 cm. To increase the signal to noise ratio and reduce exposure time, the beam size should be large. With the projection effect to be taken into account, the size of the SF should be larger than the beam size, and also the PF should be larger than the SF. The beam size is primarily limited by the budget.

Third, the positioning accuracy should be better than one arcsecond. We define the positioning accuracy as the minimum angular distance we can move relative to the previous position. For spectral observations, the positioning accuracy is required to be comparable to the seeing. Since the best seeing at the SAO is approximately $0.7''$ during the night, the expected seeing during the day may be a little worse than $1''$. For that reason, we require positioning accuracy of about $1''$ for an observing duration of one hour.

Fourth, the available observational time should be sufficiently long. The sunlight is blocked by the SF when the declination of the Sun is less than zero (see Figures 10–12 in Mills 1985). In addition, the sunlight can also be blocked by the neighboring night dome. To avoid this, many coelostats are placed on a stage which can move from east to west or vice versa. In other cases, part of the PF is positioned either on the east or west side to minimize the blocked time.

Fifth, minimization of the number of moving parts is recommended. If we design the coelostat to have many motors, it would be difficult to design and control, and also errors associated with each part would accumulate. Furthermore, the cost will increase, and it would take longer time to develop the control system for driving the coelostat.

These five requirements are summarized in Table 2. Among the three types of coelostats, the vertical type uses the smallest deck space, but it is impossible to develop since an additional hole is needed to insert the pillar of the SF. For the case of the horizontal type, the required rail length must be longer than 1.5 m, making it difficult to be installed in the solar dome. For that reason, we choose the slope type coelostat.

Table 2
The requirements of the SNUC

Requirement	Value
Horizontal size	≤ 1.5 m
Beam size	≤ 0.3 m
Positioning accuracy	$\leq 1''$
Observable duration	≥ 2 hr
Minimize the number of motors	Small enough

While most coelostats move from east to west during the afternoon in order to avoid blocking the sunlight from the SF, our coelostat is fixed at the east side to decrease the number of driving parts and cost. The fixed slope frame (purple line) is shown in Figure 3.

3.2. Mathematical Model

To derive the positions of the PF and SF for a given time, we use the law of reflection (Hecht 2001)

$$\hat{\boldsymbol{n}} = \frac{\boldsymbol{r}-\boldsymbol{i}}{|\boldsymbol{r}-\boldsymbol{i}|}\,, \tag{1}$$

$$\boldsymbol{r} = \boldsymbol{i} - 2\,(\boldsymbol{i}\cdot\hat{\boldsymbol{n}})\,\hat{\boldsymbol{n}}\,, \tag{2}$$

where $\hat{\boldsymbol{n}}$ is the normal vector of a plane mirror, $\boldsymbol{i}$ is the vector of the incident light, and $\boldsymbol{r}$ is the direction vector of reflected light. To solve the problem, we select a coordinate system where the origin is located at the central point of the hole, the $\hat{\boldsymbol{i}}$-direction represents east and the $\hat{\boldsymbol{j}}$ direction south (see Figure 3). The input parameters of the slope type are the lowest position of the rail of the slope $(X_p(t_0),\ Y_p(t_0),\ Z_p(t_0)) = (X_0,\ Y_0,\ Z_0)$, fixed location of the slope ($X_p = X_0 = constant$), and the height of the SF above the hole, i.e. $(X_s,\ Y_s,\ Z_s) = (0,\ 0, Z_s)$. Since the angle of the slope is eqaul to the latitude ϕ at the SAO, Z_p and Y_p satisfy the following relations

$$\begin{aligned} Z_p - Z_0 &= -\,(Y_p - Y_0)\tan\phi\,, \\ Z_p &= -\,(Y_p - Y_0)\tan\phi + Z_0\,. \end{aligned} \tag{3}$$

The normal vector of the PF is defined by the latitude and the rotated angle θ_p between the sun and south

$$\hat{\boldsymbol{n}}_p = (\sin\theta_p,\ \ \sin\phi\cos\theta_p,\ \ \cos\phi\cos\theta_p)\ , \tag{4}$$

The direction vector of the Sun is given as follows

$$\boldsymbol{d}_\odot = (-\cos h\sin A,\ \ -\cos h\cos A,\ \ \sin h)\ , \tag{5}$$

where h is the altitude, and A is the azimuthal angle of the Sun. Since the incident vector $\boldsymbol{i}_p$ is opposite in direction to the Sun, i.e., $\boldsymbol{i}_p = -\boldsymbol{d}_\odot$, the reflected vector from the PF is given as follows

$$\boldsymbol{r}_p = -\boldsymbol{d}_\odot + 2\,(\boldsymbol{d}_\odot\cdot\hat{\boldsymbol{n}}_{\boldsymbol{p}})\,\hat{\boldsymbol{n}}_{\boldsymbol{p}}\,. \tag{6}$$

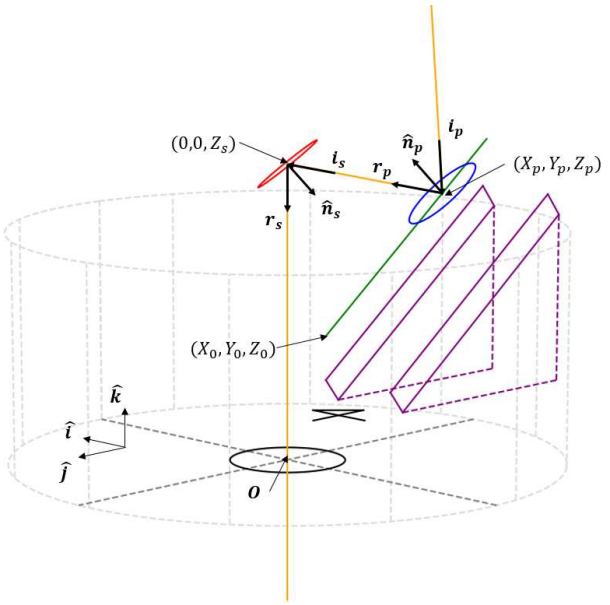

Figure 3. The 3-dimensional conceptual design of the SNUC. The blue and red circles represent the PF and SF respectively. The orange line is the lightpath, and the green line is the path of PF on the slope which is represented in purple. All relevant vectors and parameters are shown in this figure.

Since the reflected light should travel to the SF from the PF, the direction vector of the reflected light is given by

$$\boldsymbol{r}_p = -\frac{1}{l}\left(X_p, Y_p, Z\right) , \tag{7}$$

such that the rotated angle and position of the PF is given by solving the simultaneous equations

$$\theta_p = \frac{1}{2}\left[\sin^{-1}\left(\frac{e}{b^2+c^2}\right) - \alpha\right] , \tag{8}$$

$$l = \frac{X_p}{a\sin 2\theta_p - \cos h \sin A \cos 2\theta_p} , \tag{9}$$

$$\begin{aligned} Y_p = & -l(-\cos h \cos A + a \sin\phi \\ & + \cos h \sin A \sin\phi \sin 2\theta_p \\ & + a \sin\phi \cos 2\theta_p) , \end{aligned} \tag{10}$$

where the parameters a to e and α are,

$$a = \cos h \cos A \sin\phi - \sin h \cos\phi , \tag{11}$$

$$b = \cos h \sin A \left(\cos\phi + \sin\phi \tan\phi\right) - af , \tag{12}$$

$$c = a\left(\cos\phi + \sin\phi\tan\phi\right) + f\cos h \sin A , \tag{13}$$

$$\begin{aligned} e = & -\sin h - a\left(\cos\phi + \sin\phi\tan\phi\right) \\ & + \cos h \cos A \tan\phi , \end{aligned} \tag{14}$$

$$\alpha = \tan^{-1}\left(\frac{c}{b}\right) , \tag{15}$$

with

$$f = \frac{-Z_s + Z_0 + Y_0 \tan\phi}{X_p} . \tag{16}$$

The angle of the SF between the normal vector $\hat{\boldsymbol{n}}_s$ and reflected vector $\boldsymbol{r}_s$ is derived easily. The $\boldsymbol{r}_p$ vector which is reflected by the PF is eqaul to the incident light vector to the SF, i.e., $\boldsymbol{i}_s = \boldsymbol{r}_p$, and it is reflected to the hole, $\boldsymbol{r}_s = (0,\ 0,\ -1)$. As a result, the rotated angle of the SF is given as follows

$$\theta_s = \cos^{-1}\left(\hat{\boldsymbol{n}}_s \cdot \boldsymbol{r}_s\right) , \tag{17}$$

$$\hat{\boldsymbol{n}}_s = \frac{-\boldsymbol{r}_p + \boldsymbol{r}_s}{|-\boldsymbol{r}_p + \boldsymbol{r}_s|} , \tag{18}$$

The solutions of these equations for four different times are shown in Figure 4, and Table 3 summarizes the initial conditions and results. Input values of the positions of PF and SF are X_p = -60 cm, Y_0 = 20 cm, Z_0 = 90 cm and Z_s = 160 cm. In Figure 4, the sunlight (orange line) is first reflected by the PF (blue circle) and redirected to the lower laboratory by the SF (red circle). The slope frame represented in purple is located at the north side inside the dome (gray dotted line). Each day, the SF is fixed but the PF is rotated along the polar axis, which is parallel to the inclined plane of the slope (see panels a to c). The green line represents the artificial path of the PF on the slope, which includes the margin for the mount. The panels (b) and (d) clearly show the annual change of the position of the PF on the slope and the angle of the SF. At the summer solstice, the PF is located at the top of the slope (panel b) and is at the lowest level at the winter solstice (panel d). As mentioned in Section 3.1, the height of the SF is not changed at any time, and the EW position of the slope is fixed to the east side.

Table 3
Parameters of conceptual design of the SNUC

Parameter	Value
Type	Slope
Length of the rail	$\geq$ 130 cm
Stroke of the rail	65 cm
Diameter of the PF	ϕ 45 cm
Initial position of the PF	(−60, 20, 90)
Diameter of the SF	ϕ 39 cm
Position of the SF	(0, 0, 160)
Observable time	$\geq$ 3 hrs

The sizes of the two mirrors are fixed by the requirement for the beam size. Due to the effect of projection, the reflected beam size decreases by a factor of $\cos\theta$, where the θ is the angle between two planes. To satisfy our requirements, the length of the semiminor axis of the final reflected beam should be longer than 30 cm for all times. Hence, the shortest size of the PF and SF are 45 cm and 39 cm respectively. Although the proposed type of coelostat is different from the one used by KASI, the size of the two mirrors are similar (Park et al. 2003). If we assume that the length of the mount is 1.5 times longer than the diameter of the PF, the required length of the rail will be 130 cm as the calculated moving distance of the PF from the winter solstice to summer solstice is 65 cm. This is the stroke of the rail.

Since we fix the slope frame on the east side of the

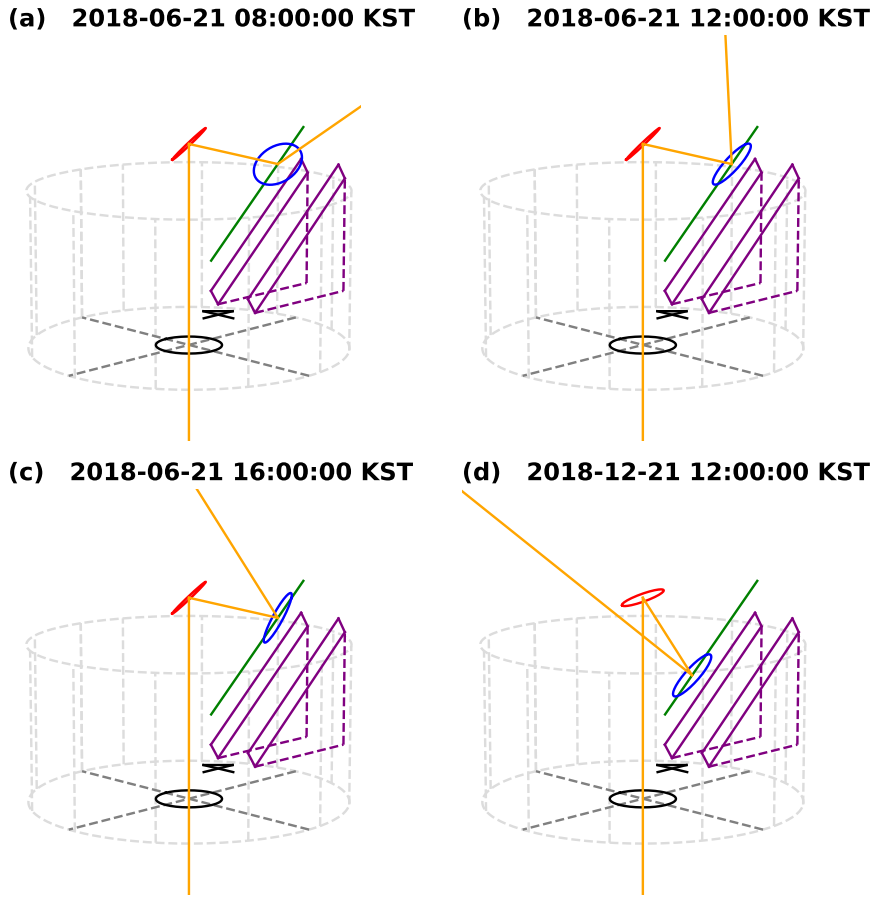

Figure 4. The conceptual design of the SNUC for four different times. The panels from (a) to (c) show the rotation of PF at different times during a day in the summer. The panel (d) represents the positions of PF and SF during the winter season.

dome, the sunlight is blocked by the SF, wall, night dome and a mountain for a specific time. The results of a numerical simulation of the observable time in which the screening of the sun is less than 50% is shown in Figure 5. The observable time is represented as a white region, and the shading time is colored blue. In the morning the sunlight is mainly screened by the mountain and the wall of the dome. Such screening could be avoided if both the PF and SF could be elevated. This elevation, however, is not possible because they must be confined to the dome. In the afternoon, sunlight is mainly blocked by the SF. When the declination of the Sun becomes high, the observable time is large, and we can observe the Sun for an entire day during the summer as the Sun is not blocked by the SF. Even though the Sun has the lowest value of meridian altitude at the winter solstice, the observable duration is at least 3 hours.

3.3. Driving Components

While telescopes often utilize an AC servo motor, the SNUC adopts direct drive motors (DD motors) to rotate the mirrors. Compared to an AC servo motor with reduction gear, which is generally used in the mounting system of telescopes, the DD motor has benefits on its resolution ($< 1''$), torque (> 3 N m), and compact volume since it combines with the gear and the rotary encoder. The main advantage of the DD motor is that it has no backlash, which can cause positioning error. Therefore, the DD motor can satisfy the positioning accuracy required of the SNUC while occupying only a compact space. The home position of the DD motor is $\theta_p = 0$. The motor stops when the Sun is screened by the SF (see Figure 5) or the altitude of the sun is less than 10°.

Since the declination is controlled by transferring the PM on the slope, we convert the required positioning accuracy from arcseconds to length units. The positioning accuracy for declination is given as follows

$$r = \frac{l_s}{2 \times \theta_t} = 3.8\ \mu\text{m}/\ '', \tag{19}$$

where the stroke of the rail l_s is 65 cm and the axial tilt of the earth θ_t is 23.5°.

Since the change of the solar declination is maximized during an equinox and the calculated transferring distance d_{max} per hour is 0.4 mm/h, the tolerance ϵ_{tol} of the positioning error per hour is

$$\epsilon_{tol} = \frac{r}{d_{max}} = \frac{2850\ \mu\text{m}}{300\ \text{mm}}. \tag{20}$$

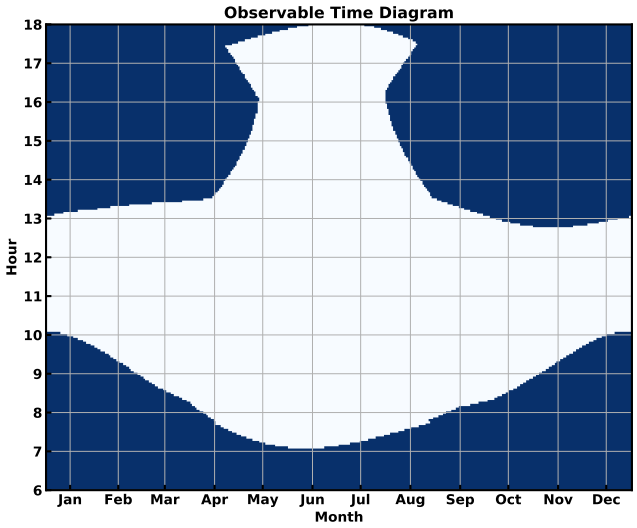

Figure 5. The observable time diagram for SNUC in the solar dome at the SAO. The white represents the available time to observe the sun, but the sunlight is blocked in the blue region.

To steer and sustain the PF on the slope while satisfying this requirement, the transfering module of the SNUC consists of a ball screw, linear motion guide (LM guide), AC servo motor and helical type reduction gear. The ball screw and LM guide are verified tools to lift payloads without crooking within industry, with high transferring accuracy, $\leq$ 30 μm/300 mm. In general, the ball screw is rotated by an AC servo motor, but the rated torque of the servo motor may not be sufficient in our case. To supplement the deficient torque, it is optimal to add helical type gear to the motor. The home position of the rail is set to the lowest position of the rail, i.e., (X_0, Y_0, Z_0). Other driving motors which are also installed in the laboratory, such as a motor to control the focusing mirror, will be described in a subsequent paper.

4. PROTOTYPE DESIGN

Even though the driving parts have a higher accuracy than our requirement, they can be affected by variations of the temperature and humidity. For example, the encoder of the DD motor made from stainless steel has thermal expansion given as follows

$$\begin{aligned} \Delta\theta &= \alpha_T \times \theta \times \Delta T\,, \\ &= 1.2'' \left(\frac{\theta}{15^\circ}\right)\left(\frac{\Delta T}{3\,\mathrm{K}}\right) \end{aligned} \tag{21}$$

where α_T is the coefficient of thermal expansion 15×10^{-6} K^{-1}, ΔT is the temperature change, and θ is the rotating angle. Thus, this thermal expansion is comparable TO our requirement of positioning accuracy during the observing time. To test these environmental effects, we designed a prototype for the PF part as shown in Figure 6. The mount part of the PF is represented in gray, and the slope part is black. To reduce the weight of the PSNUC, most parts are made of aluminum, except for the driving parts; the weight of the mount is 25 kg and the slope frame is 70 kg. The designed length of the rail is approximately 100 cm with 50 cm stroke, and the distance between two rails is about 15 cm. The length of the mount is approximately 39 cm, and the height from bottom to shaft is 19 cm.

The mount segment consists of a 20 cm plane mirror, and a DD motor. The DD motor is installed directly above the mirror shaft, and the rotation axis of the PF lies on the mirror surface, so that it is easy to trace the Sun. Since the resolution of the DD motor is 4,320,000 counts/rev, the postioning accuracy of the DD motor is 0.″3. The positioning accuracy for one hour is approximately 0.″85, since the accuracy per half rotation is roughly 10″. Information on the rotated angle of the motor is recorded by the encoder built into the DD motor, and we intend to analyze this data to complement the accuracy of the SNUC.

The slope frame is divided into three sub-segments, bottom plate, slope, and rail support. The bottom plate supports the whole PSNUC and sustains the moment using six level feet. To align the pole, the angle of the slope is designed to have the same value as the latitude of the SAO (37.4°). For the transferring motion, the ball screw, LM guides, servo motor and gear are installed in the rail support, and also the stainless tape of the linear encoder is attached to the right side. The linear encoder head is installed the right side of the mount, and it records the output transferring distance. Data recoreded by the linear encoder will be compared to the input value which is recorded by the rotary encoder in the servo motor.

To sustain and stably transfer the mount to the appropriate position, we have selected the ball screw and LM guide. From equation M29 of HIWIN (2016), the root diameter of the ballscrew should be larger than 5 mm in our case, but we select the 10 mm ball screw by considering a safety factor of 20. Specifically, we select the C5 class ball screw which has a lead accuracy a_{lead} of about 18 μm per 300 mm. The lead accuracy of the C5 class ball screw is converted to positioning error per hour, err_{track}

$$err_{track} = \frac{a_{lead}}{\epsilon_{tol}} = 0.04''/\mathrm{h}\,, \tag{22}$$

where ϵ_{tol} is the tolerable transferring error given in Equation (20).

The driving torque to rotate the ball screw is given by (HIWIN 2016)

$$T_a = \frac{F_b \times l}{2\pi\eta_1} = 0.09\ \mathrm{N\,m}\,, \tag{23}$$

$$T_b = \frac{0.3 \times l \times F_b/2.8}{2\pi} = 0.02\ \mathrm{N\,m}\,, \tag{24}$$

$$\begin{aligned} T_c &= J\alpha \\ &= 5.46 \times 1^{-5}\ \mathrm{kg\,m^2} \times 0.025\ \mathrm{m\,s^{-2}} \\ &= 6.8 \times 10^{-4}\ \mathrm{N\,m}\,, \end{aligned} \tag{25}$$

$$T = T_a + T_b + T_c = 0.11\ \mathrm{N\,m}\,, \tag{26}$$

Figure 6. Prototype design of the primary part of the SNUC.

where T_a is the driving torque for common transfer, T_b is the pre-load drag torque, T_c is the driving torque during acceleration, T is the total torque, F_b is the weight of the load, and l is the lead of the ball screw, which is approximately 2 mm for the PSNUC. Accounting for vibration and external impact, we try to choose a servo motor which has 5 to 10 times higher torque than above, but the general servo motor has less than 0.5 N m torque. For this reason, we reinforce the torque by attaching a 1/5 ratio helical type gear to the servo motor.

Since our selected servo motor has 2^{17} ppr encoder resolution r_{AC}, the positioning accuracy in length unit A is given by

$$\begin{aligned} A &= \frac{l}{2\pi} \times \frac{2\pi}{r_{AC}} R\,, \\ &= 3.1 \times 10^{-3}\ \mu\mathrm{m}\,, \end{aligned} \tag{27}$$

where the ratio R of the reduction gear is 1/5. The transferring error occurred by the 5′ backlash of the reduction gear is about 0.46 μm, and this is converted into the 0.″12 positioning error, which is tolerable to our requirement. We plan to check this error by using the linear encoder which has 0.5 μm accuracy, and this value is similar to the calculated error of the transferring module.

Since the balls of the ball screw and LM guide may begin to wear, we cannot use the PSNUC permanently. Generally, the lifetime of the LM guide is much longer than the the ball screw, so the expected lifetime of the PSNUC is determined by the ball screw. The calculated life cycle of the ball screw is about 2.85×10^8 revolutions (HIWIN 2016), and this can be written in time units as

$$\begin{aligned} L &= \frac{L_{rev}}{(l_s/l) \times 2 \times N}\,, \\ &= \frac{2.85 \times 10^8}{(650/2) \times 2 \times 100} \times \frac{1}{365}\ \mathrm{yrs}\,, \\ &\approx 12\ \mathrm{yrs}\,, \end{aligned} \tag{28}$$

where L_{rev} is the life cycle in the unit of a revolution, l_s is the stroke, l is the lead of ball screw, and N is the number of repetitions for a day, which is set to 100. This lifetime is 10 times longer than the test duration which is approximately one year. The lifetime of the SNUC is expected to be longer than the PSNUC as we lift the PF up and down only once per observation, so the actual repetition will beis 2 per day. The specifications of the PSNUC are summarized in Table 4.

Table 4
Parameters of the PSNUC

Parameter	Value
Diameter of the mirror	20 cm
Size of the mount	39 cm×15 cm×19 cm
Length of the rail	100 cm
Stroke of the rail	50 cm
Inclination of the slope	37.4°
Weight of the mount part	17 kg
Weight of the slope frame	70 kg
Lead of the ball screw	0.2 cm
Lead accuracy of ball screw	18 μm / 300 mm
Resolution of the servo motor	2^{17} ppr
Ratio of the gear	1/5
Backlash of the gear	5′
Positioning accuracy of DD motor	0.″3
Positioning accuracy of rail	0.″12
Lifetime of the PSNUC	12 yrs

5. Summary and Plan

The solar group at SNU is undertaking a project to develop a coelostat, which is planned to be installed in the SAO. The structure of the solar dome constrains the coelostat to be compact; we therefore select the slope type coelostat fixing the slope frame to the east side. Even though the primary mirror is designed to be fixed on the east side, we can continuously observe the Sun for an entire day during the summer season and at least 3 hours at the winter solstice. The design sizes of the two mirrors of the SNUC are 45 cm for the PF and 39 cm for the SF. Considering the size of the mount of the PF, the length of the sloped rail is 130 cm with a stroke of 65 cm. The driving components of the SNUC are designed to have high positioning accuracy ($< 1''$). This high accuracy coelostat provides an opportunity for students to observe a high-resolution solar spectrum as well as a real-time solar image. Students can also use it to test new generatios of optical instruments, which will be developed by them.

To avoid mistakes in the designing phase and to test the environmental effects, we designed a prototype

for the primary mirror part. The PSNUC has a 20 cm plane mirror and 1 m sloped rail with 50 cm stroke. The driving components of the prototype have less than 2″ accuracy. The expected lifetime of the PSNUC is approximately 12 years.

We intend to perform the environmental test in 2019. The temperature and humidity will be controlled by thermo-hygrostat in the laboratory, and the variations of these inside the prototype will be measured by a single board computer. The output position of the mount will be recorded by the linear encoder and will be compared with the input data. The control program to steer the PSNUC will be deveoped during 2018 using the Visual C++ computational language.

ACKNOWLEDGMENTS

We are grateful to the referees for constructive comments. This work was supported by the Korea Astronomy and Space Science Institute under the R&D program, Development of a Solar Coronagraph on International Space Station (Project No. 2017-1-851-00), supervised by the Ministry of Science and ICT. This work was supported by the space fusion education track program in SNU. We gratefully acknowledge the support of METASPACE.

REFERENCES

D'Alessio, F., Faccini, M., Leoni, R., & Giobbi, G. 2012, The Solar Tower at Monte Mario: a New Didactic Laboratory for Astronomy, Memorie della Societa Astronomica Italiana Supplementi, 19, 406

Dreyer, O., Ippa, A., Seubert, S., et al. 2014, Performance Verification of the DKIST Mount and Coudé Laboratory, Proc. SPIE, 91452A

Dunn, R. B. 1985, High Resolution Solar Telescopes, Sol. Phys., 100, 1

Han, H.-J., Selkowitz, S., Oh, S.-J., & Chun, W. 2014, An Analysis on the Energy and Daylighting Efficiencies of Rehabilitated Linde-Robinson Laboratory: Solar Telescope Daylighting with Coelostat, JKSES, 34, 53

Hecht, E. 2001, Optics, 4th edition (Boston: Addison-Wesley), 97

HIWIN Technologies Corp. 2015, Ballscrews Technical Information, 20th edition (Taichung: HIWIN Technologies Corp.), 22 (https://www.hiwin.com/pdf/ballscrews.pdf)

Kim, Y. H., Moon, Y. J., Cho, K. S., et al. 2006, Development of KASI Solar Imaging Spectrograph, PKAS, 21, 51

Livingston, W. C., Harvey, J., Pierce, A. K., et al. 1976, Kitt Peak 60-cm Vacuum Telescope, Appl. Opt., 15, 33

Maurya, R. A., Chae, J., Park, H., et al. 2013, Chromospheric Sunspot Oscillations in Hα and Ca II 8542 Å, Sol. Phys., 288, 73

Mills, A. A. 1985, Heliostats, Siderostats, and Coelostats: A Review of Practical Instruments for Astronomical Applications, J. Brit. Astron. Assoc., 95, 89

Nah, J.-K., Chae, J.-C., Park, Y.-D., et al. 2011, Development of the Fast Imaging Solar Spectrograph for 1.6 m New Solar Telescope, PKAS, 26, 45

Park, Y. D., Cho, K. S., Moon, Y. J., et al. 2003, Development of Mid-Resolution Solar Spectroscopic System, PKAS, 18, 61

Stix, M. 2004, The Sun: An Introduction (Berlin: Springer), 87